The involvement of ACO3 protein in diabetic retinopathy through the PI3k/Akt signaling pathway

*Yi Zhang[A,B,D,F], *Wenjun Wang[B,C,F], Anhuai Yang[A,E,F]

Eye Center, RenMin Hospital of Wuhan University, China

A – research concept and design; B – collection and/or assembly of data; C – data analysis and interpretation;
D – writing the article; E – critical revision of the article; F – final approval of the article

Address for correspondence
Anhuai Yang
E-mail: yah0525@126.com

* These two authors contributed equally to this work.

Abstract

Background. Diabetic retinopathy (DR) is one of the most common complications of diabetic microvascular disease and its pathogenesis is complicated. The PI3k/Akt signaling pathway plays an important role in the angiogenesis of DR.

Objectives. To explore the molecular mechanisms of the ACO3 protein and related proteins in DR, in order to provide a scientific theoretical basis for the clinical treatment of this disease.

Materials and methods. A DR rat model was used in this study. One group (anti-ACO3 group, n = 10) was injected with protein ACO3 antagonist; the 2nd study group (the DR group, n = 10) was injected with the same amount of normal saline; the control group (n = 10) did not undergo any procedures. We used hematoxylin and eosin (H&E) staining to observe the pathological features of the eye tissues. Immunohistochemistry was used to analyze the expression of ACO3 and AKT. Western blot was used to analyze the expression of ANGPT1, ANGPT4 and KDR; reverse transcription polymerase chain reaction (RT-PCR) was used to assess the mRNA expression of AKT, ACO3 and SMOX in the eye tissues of the rats.

Results. In the anti-ACO3 group, the results of H&E staining showed that there was a decrease in retinal edema and no obvious abnormality in the blood vessels. The immunohistochemistry analysis of proteins proved that ACO3 and AKT were strongly expressed in the DR group. The western blot analysis of ANGPT1, ANGPT4 and KDR expression showed that in the DR group, the expression of all 3 proteins was higher than in the anti-ACO3 group, and much higher than in the control group.

Conclusions. The mRNA expression of *AKT*, *ACO3* and *SMOX* was strong in the DR group, but decreased in the anti-ACO3 group.

Key words: diabetic retinopathy, mechanism, ACO3, PI3k/Akt signaling pathway

408

Y. Zhang, W. Wang, A. Yang. ACO3 in DR via the PI3k/Akt signaling pathway

Background

Along with social and economic development, improved living standards and changes in eating habits, diabetes has become a common disease affecting people's health and life. Diabetic retinopathy (DR) is one of the most universal complications of diabetic microvascular disease, often causing serious visual impairment.[1] According to the research conducted by the World Health Organization (WHO), the number of diabetic patients in the world reached 366 million cases in 2011, and by 2025 this number will exceed 500 million.[2] It was recently reported that the global morbidity of DR was 34.6%, while in developed countries it was nearly 40.3%.[3] The number of patients with DR in China has been reported to be as high as 13.16 million.[4] The most common features of DR patients include decreased vision, microhemangioma, bleeding spots, hard exudate, retinal neovascularization, venous beading, and macular edema.[5,6] In some severe cases, vitreous hemorrhage, fibrogenesis and retinal angiogenesis have been noted, which might cause neovascular glaucoma or retinal detachment.[7] If effective treatment measures are not taken in time, retinal cell death and fibrosis are likely to occur, resulting in a permanent loss of vision. Therefore, an early and accurate diagnosis and treatment of DR is particularly important.[8]

The pathogenesis of DR is complicated. It is related to glucose metabolism, growth hormone and angiogenic growth factors. In terms of glucose metabolism, when blood glucose level is elevated, the osmotic pressure inside cells is higher than that of the outside cells due to the failure of glycolysis, leading to an imbalance of water electrolytes in eye cells.[9,10] Retinal microvascularization would interfere with the metabolism of inositol and accumulate advanced glycation end products (AGEs) under the stimulus of long-term high-sugar environment. At the same time, this process affects the activity of Na^+/K^+-ATPase in cells; increases the permeability of capillaries; thickens the basement membrane; narrows capillary lumens; increases retinal ischemia, hypoxia and the release of vascular proliferation factors; and promotes the formation of new blood vessels.[11]

As one of the important pathways involved in endothelial cell migration, proliferation and vascular dysfunction, the PI3k/Akt signaling pathway also plays an important role in the process of DR neovascularization.[12] Among proteins related to PI3k/Akt signaling pathway, the ACO3 protein is involved in regulating cell proliferation and inducing neovascularization.

Objectives

The aim of the study was to explore the molecular mechanisms of the ACO3 protein and related proteins in DR, in order to provide a scientific theoretical basis for the clinical treatment of this disease.

Materials and methods

The study used 30 Wistar rats (purchased from Harbin Medical University, China); streptozotocin (STZ; Sigma-Aldrich, St. Louis, USA); ACO3 antagonist (Thermo Fisher Scientific, Waltham, USA); hematoxylin (Invitrogen, Carlsbad, USA); phosphate-buffered saline (PBS) (0.1 m, pH 7.0); TRIzol RNA agent; 6-, 12- and 48-plate cell culture dishes (Thermo Fisher Scientific); 5 mL and 10 mL sterile pipettes (Corning, New York, USA); 10 μL, 20 μL, 200 μL, and 1000 μL transfer pipettes (Eppendorf, Enfield, USA); 10 mL and 50 mL centrifuge tubes (Thermo Fisher Scientific); a conventional polymerase chain reaction (PCR) instrument (Agilent Technologies Inc., Santa Clara, USA); western blotting instruments (Eppendorf AG, Hamburg, Germany); a confocal microscope (Olympus Corp., Tokyo, Japan); a LKB-V ultra-thin slicer (JEOL Ltd., Tokyo, Japan); and a Jem-2000EX fundus fluorescein angiograph (JEOL Ltd.).

Rat model of diabetic retinopathy

We divided 30 Wistar rats (8–9-week old) into 3 groups of 10 rats each. One was the control group, while the other 2 were used to establish the DR model. Twenty rats were randomly assigned to the 2 model diabetic groups. These rats were administered STZ (60 mg/kg) by intraperitoneal injection to induce diabetes. Their fasting glucose was monitored and glucose level ≥16.65 mmol/L was considered the standard model. After 1 month, the diabetic rats were injected with 0.05 μg of vascular endothelial growth factor (VEGF), 2 mm behind the temporal limbic cornea using a microinjector. It passed through the ciliary body and entered the vitreous cavity. The injection was done slowly to keep the needles in for 10 s, in order to create a model of ophthalmic lesions in proliferative diabetes mellitus. The fundus changes in the rats were examined to judge whether the DR model had been successfully constructed. One DR group (called anti-ACO3 group) was injected with 5 μL of ACO3 antagonist (10 μg/mL); the other DR group (called DR group) was injected with the same amount of saline in vitreous body.

Fundus fluorescein angiography

Fundus fluorescein angiography (FFA)[13] was carried out as follows: before the examination, 1 mL of 1% fluorescein sodium was injected intravenously for an allergy test, and was observed for 15 min to ensure that there was no abnormal reaction. Then, 5 mL of 10% fluorescein sodium was immediately injected into each rat and 1 eye was selected as the main eye. After 10–15 s of injection, the early image was shot continuously. After 1–10 min of injection, the middle image was shot. After 10 min, the late image was shot and stored for analysis.

H&E staining to examine the pathological features of the eye tissues

Eye tissues were taken from the 2 DR groups and the control group, and hematoxylin and eosin (H&E) staining was used to examine the pathological features of the tissues.[14] Four weeks after the administration of the ACO3 antagonist or saline to the diabetic rats, pentobarbital sodium was injected intraperitoneally for anesthesia and the retinal tissues of the rats were taken. The tissues were fixed with 4% paraformaldehyde and decalcified with 15% ethylenediamine tetraacetic acid (EDTA) at room temperature. After dehydration, the retinal tissues were embedded in paraffin and 4-μm tissue sections were prepared for pathological observation. The section samples of the 3 groups of rats were stained and dewaxed with xylene twice. Then, the samples were hydrated with gradient ethanol for 3 min and stained with hematoxylin for 5 min. The tissues were then rinsed with 1% hydrochloric acid-ethanol for 30 s, followed by reflux treatment in 0.2% ammonia for 2 min, stained with 0.5% eosin for 10 min, and washed with water once. Gradient ethanol was used for dehydration treatment, and finally, neutral gum was used for sealing. The image was analyzed using an optical microscope.

Immunohistochemistry analysis of ACO3 and AKT expression

Immunohistochemistry staining was used to detect the expression of ACO3 and AKT in the eye tissues.[15] The paraffin-embedded islet tissue of the rats was sectioned at a thickness of 4 μm. The two-step immunohistochemistry method was used for staining. The tissue sections were roasted at 65°C for 12 h, dewaxed and hydrated. Endogenous peroxidase was inactivated by 3% hydrogen peroxide, and the specimens were washed twice with PBS. Mouse anti-human primary antibody ACO3 and AKT were added and washed twice with PBS. Next, the streptomycin working solution (labeled with horseradish peroxidase (HRP)) was added and incubated at 37°C for 25 min. Then, it was washed with PBS, stained with hematoxylin and sealed with neutral chicle.

Western blot analysis of ANGPT1, ANGPT4 and KDR expression

Total proteins were extracted from the eye tissue and blood vessels of each group of rats, and 20-μg protein samples were prepared. We used 5% concentrated gel and 12% isolated gel to isolate proteins using sodium dodecyl sulphate–polyacrylamide gel electrophoresis (SDS-PAGE).

Objective and internal proteins were transferred to nitrocellulose (NC) membranes, then sealed with 5% skimmed milk powder sealing fluid for 2 h at room temperature. Rat anti-human primary antibody ANGPT1 (1:500), rat anti-human primary antibody ANGPT4 (1:500), rat anti-human primary antibody KDR (1:500), and rat anti-human primary antibody β-actin (1:1000) were added and incubated overnight at 4°C. The specimens were washed 4 times in Tris-buffered saline with Tween (TBST), and HRP-labeled sheep anti-rat secondary antibody (1:5000) was added and incubated at 37°C for 1 h. The specimens were again washed 4 times in TBST. Color was developed with enhanced chemiluminescence (ECL) solution; protein bands were exposed using ECL blotting detection reagent (Beyotime, Shanghai, China); and the images were photographed and analyzed quantitatively. The experiment was repeated 3 times.

RT-PCR analysis of *AKT*, *ACO3* and *SMOX* mRNA expression

The analysis of *AKT*, *ACO3* and *SMOX* mRNA expression was conducted as described by Rouhani et al.[16]: total RNA was extracted with TRIzol reagent (Shanghai Pufei Biotech, Shanghai, China), according to the manufacturer's instructions. Nucleic acid-protein complexes were extracted with chloroform and precipitated in isopropanol. The complexes were cleaned using 75% ethanol and purified with RNase-free water. The expression level of *GAPDH* was selected as the internal reference. Primers for PCR detection were designed and synthesized according to the information of the target gene sequences, as shown in Table 1. The amplifications were performed in a 96-well plate at 95°C for 10 min, followed by 40 cycles of 95°C for 15 s and 60°C for 1 min. Each sample was run in triplicate. The relative miRNA-126 and mRNA expression was expressed using the $2^{-\Delta\Delta Ct}$ method.

Statistical analyses

One-way analysis of variance (ANOVA) followed by Tukey's post hoc test were used to analyze the data for comparison among 3 groups. The variance homogeneity was tested using Levene's variance homogeneity test. The distribution of the data was analyzed with Kolmogorov–Smirnov and Shapiro–Wilk method, and normally distributed data were expressed as mean ± standard deviation (SD). Statistical significance was defined

Table 1. Nucleic acid sequences of polymerase chain reaction (PCR) primers

Genes	Upstream primer 5'-3'	Downstream primers 5'-3'
AKT	GAGATCACAACAGTCCACAC	AAGGTGTCCTGCAAGCTGTC
ACO3	ACTTTGAGAATGTGGCACGG	TAACATGGCCAAAGTAGGCG
SMOX	TGAGGAGCCCGATCTAGAC	AAGGTCCCAGTACCCCCTC

as $p < 0.05$. All calculation was conducted using SPSS v. 18.0 software (SPSS Inc., Chicago, USA).

Results

Rat model of diabetic retinopathy

Rats with the blood glucose value ≥16.7 mmol/L were defined as diabetic rats. Then, the diabetic rats injected with vitreous cavity were subjected to fundus fluorescein examination to observe the obvious retinal hemorrhage or exudation, telangiectasia, arteriovenous abnormalities, and other conditions in the fundus of rats, indicating that the DR model of the rats was successfully established.

Fundus fluorescein angiography

The FFA results showed that there was no significant DR and no abnormal phenomena in the control group (Fig. 1A). However, background fluorescence enhancement, vascular tortuosity and dilatation, and fluorescence leakage from neovascularization, intraretinal hemorrhage and microhemangioma were observed in the DR group (Fig. 1B). The characteristics of the eye tissue of the DR rats in the anti-ACO3 group were significantly better than

in the DR group, and the number of new microvessels was lower in the anti-ACO3 group (Fig. 1C). This indicates that the ACO3 protein is involved in regulating cell proliferation and inducing neovascularization.

H&E staining to examine pathological features of the eye tissues

The pathological histology of the retinas in all 3 groups was examined. It could be seen that the surface of the retina in the control group was smooth, and the cells in the inner and outer nuclear layer were arranged closely and orderly (Fig. 2A). In the DR group, there was obvious edema in the inner retina boundary; the cells in the inner and outer nuclear layers were not arranged neatly, and more synaptic membranes of vascular endothelial cells could be seen (Fig. 2B). However, in the anti-ACO3 group, there was a decrease in retinal edema, and loose arrangements of cells were observed only in the inner core layer (Fig. 2C).

Immunohistochemistry analysis of ACO3 and AKT expression

The expression levels of proteins ACO3 and AKT were the lowest in the control group, and were highly expressed in the DR group, as indicated by the red arrow in Fig. 3.

normal   **diabetic retinopathy**   **ACO3 protein antibody**
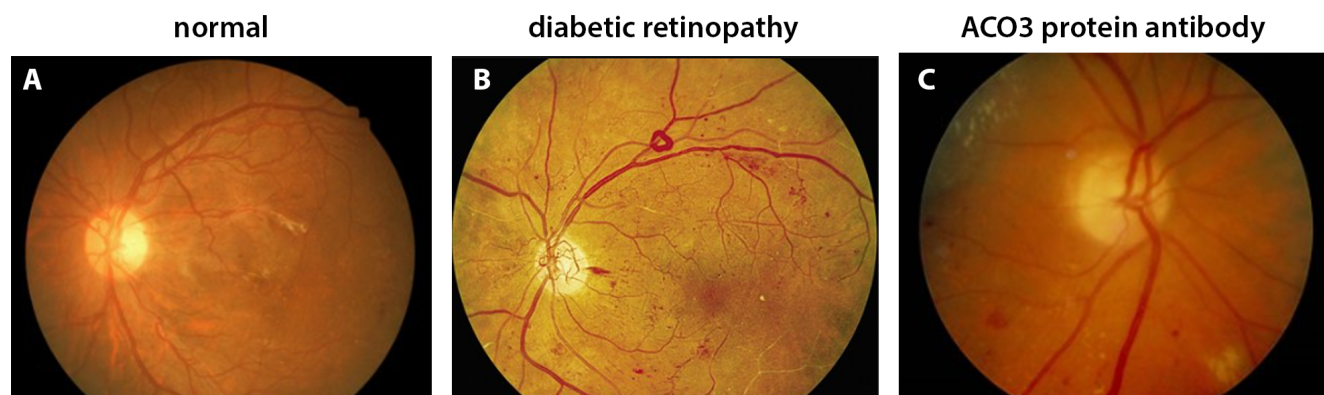
Fig. 1. Morphological characteristics of rat eye tissues observed by fundus fluorescein angiography (FFA) (×400) (n = 10). A. Control group; b. Diabetic retinopathy (DR) group; C. Anti-ACO3 group

normal   **diabetic retinopathy**   **ACO3 protein antibody**

Fig. 2. Histopathological examination of rat retinas using hematoxylin and eosin (H&E) staining (×400 magnification) (n = 10). A. Control group; B. Diabetic retinopathy (DR) group; C. Anti-ACO3 group

In the anti-ACO3 group, the expression levels of ACO3 and AKT were decreased.

Western blot analysis of ANGPT1, ANGPT4 and KDR expression

The expression levels of ANGPT1, ANGPT4 and KDR in the rat eye tissues are shown in Fig. 4. The expression of these proteins was higher in DR group than in the anti-ACO3 group (ANGPT1 $p < 0.001$, ANGPT4 $p < 0.001$, KDR $p < 0.001$, ANOVA followed by Tukey's post hoc test), and much higher than in the control group (ANGPT1 $p < 0.001$, ANGPT4 $p < 0.001$, KDR $p < 0.001$, ANOVA followed by Tukey's post hoc test). However, the expression levels of these proteins were high in anti-ACO3 group compared with the control group ($p < 0.05$). The original statistical data of western blot are shown in Table 2–5.
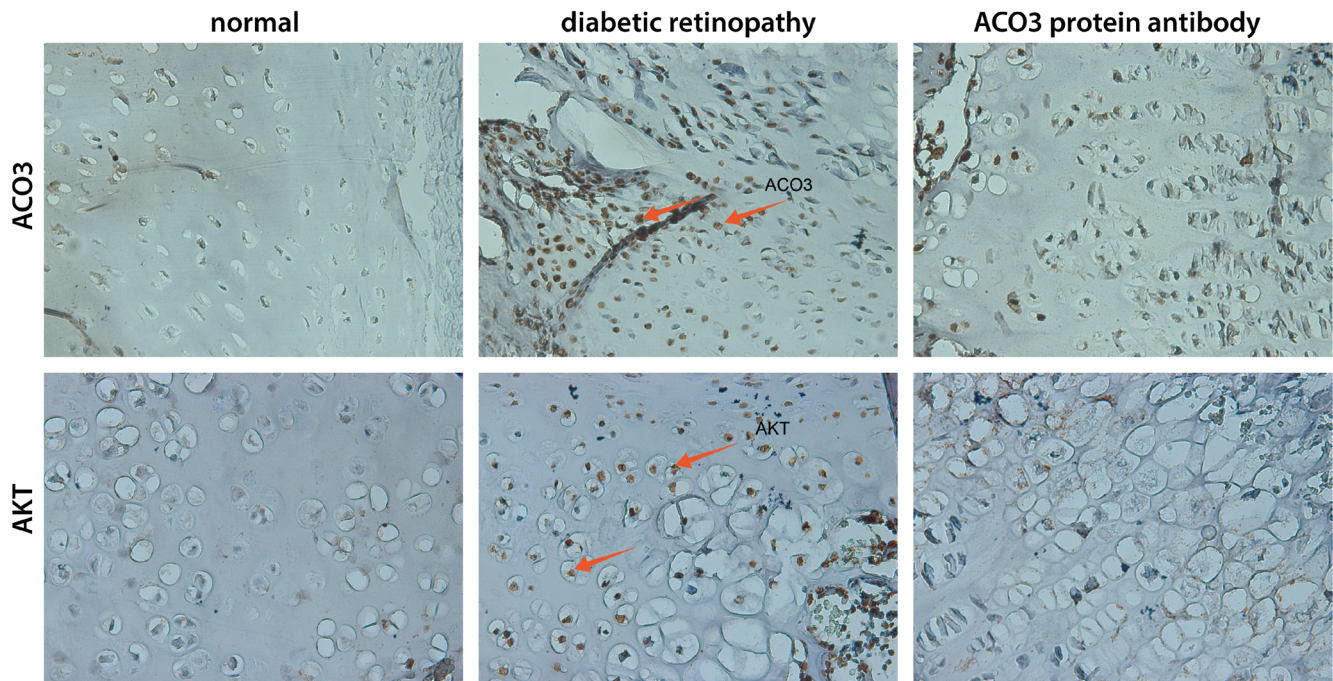
Fig. 3. Immunohistochemical analysis of the expression of proteins ACO3 and AKT in ocular tissues (×400 magnification) (n = 10). The arrows point to the positive cells
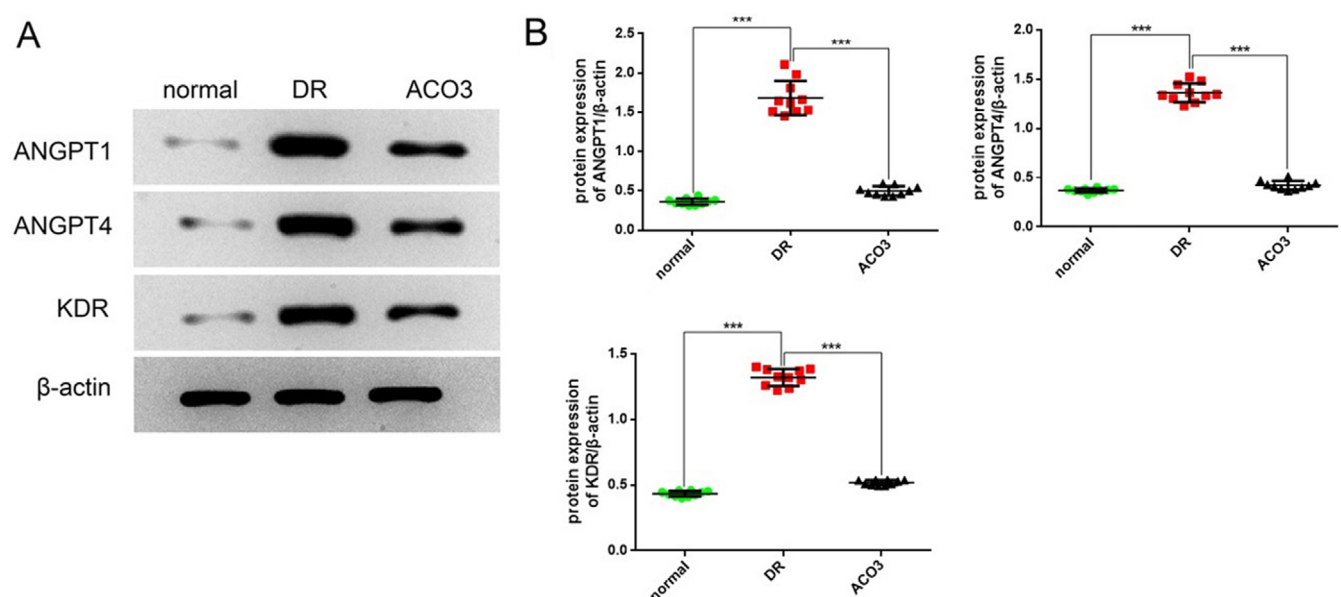
Fig. 4. Expression levels of proteins ANGPT1, ANGPT4 and KDR in different groups determined using western blot (mean ± standard deviation (SD), n = 10). A. Gray value; B. Statistical analysis; *** $p < 0.001$, compared with the diabetic retinopathy (DR) group. The statistical difference was analyzed using one-way analysis of variance (ANOVA) followed by Tukey's post hoc test

Fig. 5. The mRNA expression of *AKT*, *ACO3* and *SMOX* mRNA in eye tissues of diabetic rats (mean ± standard deviation (SD), n = 10). *** p < 0.001, compared with the diabetic retinopathy (DR) group. The statistical difference was analyzed using one-way analysis of variance (ANOVA) followed by Tukey's post hoc test
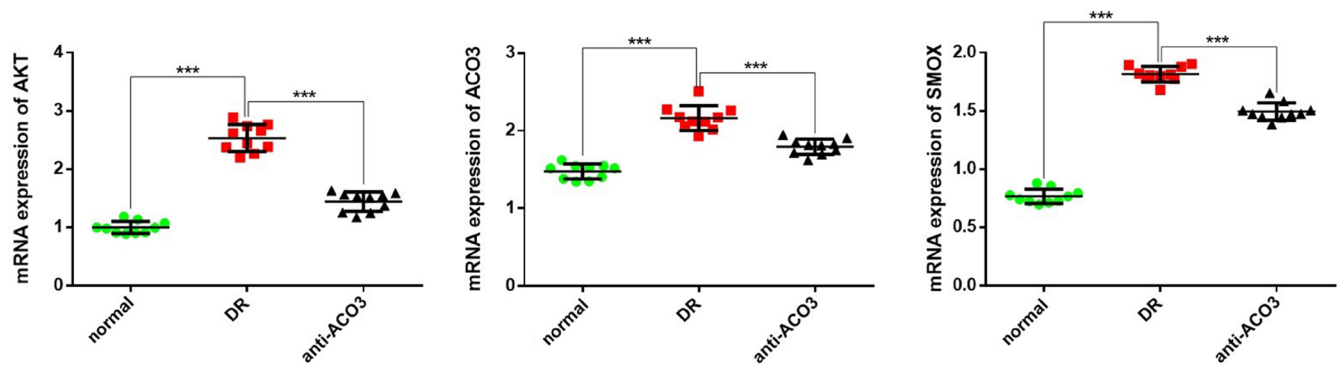
RT-PCR analysis of *AKT*, *ACO3* and *SMOX* mRNA expression

The mRNA expression levels of *AKT*, *ACO3* and *SMOX* in the DR rats with eye lesions were all increased, but were lower in the anti-ACO3 group compared with the DR group (*AKT* p < 0.001, *ACO3* p < 0.001, *SMOX* p < 0.001, ANOVA followed by Tukey's post hoc test) (Fig. 5). Cell proliferation in the DR group indicates that ACO3 is involved in regulating cell proliferation and inducing neovascularization. The ACO3 and SMOX have characteristics of mutual regulation, and synergistically participate in the regulation of amino acid metabolism and promotion of cell proliferation. The high expression levels of AKT indicate the the activation of the PI3K/Akt signaling pathway, which regulates the increase of NOS3, an enzyme related

Table 2. Description of the genes

Genes		n	Mean	Standard deviation	Standard error	95% CI lower limit	95% CI upper limit	Minimum	Maximum
ANGPT1	1.0000	10	0.360867	0.0399287	0.0126266	0.332304	0.389430	0.3124	0.4382
	2.0000	10	1.681553	0.2184303	0.0690737	1.525297	1.837808	1.4524	2.1072
	3.0000	10	0.499627	0.0599933	0.0189716	0.456711	0.542544	0.4290	0.5946
	total	30	0.847349	0.6161856	0.1124996	0.617262	1.077436	0.3124	2.1072
ANGPT4	1.0000	10	0.370262	0.0206188	0.0065202	0.355513	0.385012	0.3295	0.4037
	2.0000	10	1.362208	0.0952097	0.0301079	1.294099	1.430317	1.2285	1.5247
	3.0000	10	0.422209	0.0448262	0.0141753	0.390142	0.454275	0.3648	0.5133
	total	30	0.718227	0.4674832	0.0853504	0.543665	0.892788	0.3295	1.5247
KDR	1.0000	10	0.434405	0.0210397	0.0066533	0.419354	0.449456	0.4012	0.4606
	2.0000	10	1.319921	0.0648779	0.0205162	1.273511	1.366332	1.2217	1.4007
	3.0000	10	0.519005	0.0192815	0.0060973	0.505212	0.532798	0.4947	0.5398
	total	30	0.757777	0.4077310	0.0744412	0.605528	0.910026	0.4012	1.4007
AKT	1.0000	10	0.998226	0.1035957	0.0327598	0.924118	1.072334	0.8884	1.1859
	2.0000	10	2.532469	0.2313107	0.0731469	2.367000	2.697939	2.2005	2.8856
	3.0000	10	1.441751	0.1663498	0.0526044	1.322751	1.560750	1.1740	1.6333
	total	30	1.657482	0.6770827	0.1236178	1.404655	1.910309	0.8884	2.8856
ACO3	1.0000	10	1.474441	0.0965224	0.0305231	1.405393	1.543489	1.3439	1.6208
	2.0000	10	2.161590	0.1599465	0.0505795	2.047171	2.276008	1.9295	2.5062
	3.0000	10	1.793600	0.0985943	0.0311783	1.723070	1.864131	1.6211	1.9456
	total	30	1.809877	0.3088590	0.0563897	1.694547	1.925207	1.3439	2.5062
SMOX	1.0000	10	0.767047	0.0611052	0.0193232	0.723335	0.810759	0.6958	0.8793
	2.0000	10	1.815675	0.0661369	0.0209143	1.768363	1.862986	1.6795	1.9028
	3.0000	10	1.493892	0.0755316	0.0238852	1.439860	1.547924	1.3850	1.6525
	total	30	1.358871	0.4508948	0.0823218	1.190504	1.527238	0.6958	1.9028

95% CI – 95% confidence interval.

Table 3. Multiple comparison genes

Dependent variable	(I) groups			(J) groups		Mean D (I–J)	SE	Sig	95% CI	
									lower limit	upper limit
ANGPT1	dimension2		1.0000	dimension3	2.0000 3.0000	−1.3206857* −0.1387606	0.0593887 0.0593887	0.000 0.068	−1.467935 −0.286010	−1.173436 0.008489
		2.0000		dimension3	1.0000 3.0000	1.3206857* 1.1819251*	0.0593887 0.0593887	0.000 0.000	1.173436 1.034676	1.467935 1.329175
		3.0000		dimension3	1.0000 2.0000	0.1387606 −1.1819251*	0.0593887 0.0593887	0.068 0.000	−0.008489 −1.329175	0.286010 −1.034676
ANGPT4	dimension2		1.0000	dimension3	2.0000 3.0000	−0.9919460* −0.0519463	0.0276880 0.0276880	0.000 0.165	−1.060596 −0.120597	−0.923296 0.016704
		2.0000		dimension3	1.0000 3.0000	0.9919460* 0.9399997*	0.0276880 0.0276880	0.000 0.000	0.923296 0.871349	1.060596 1.008650
		3.0000		dimension3	1.0000 2.0000	0.0519463 −0.9399997*	0.0276880 0.0276880	0.165 0.000	−0.016704 −1.008650	0.120597 −0.871349
KDR	dimension2		1.0000	dimension3	2.0000 3.0000	−0.8855167* −0.0846002*	0.0183004 0.0183004	0.000 0.000	−0.930891 −0.129975	−0.840142 −0.039226
		2.0000		dimension3	1.0000 3.0000	0.8855167* 0.8009165*	0.0183004 0.0183004	0.000 0.000	0.840142 0.755542	0.930891 0.846291
		3.0000		dimension3	1.0000 2.0000	0.0846002* −0.8009165*	0.0183004 0.0183004	0.000 0.000	0.039226 −0.846291	0.129975 −0.755542
AKT	dimension2		1.0000	dimension3	2.0000 3.0000	−1.5342430* −0.4435245*	0.0782768 0.0782768	0.000 0.000	−1.728324 −0.637605	−1.340162 −0.249443
		2.0000		dimension3	1.0000 3.0000	1.5342430* 1.0907186*	0.0782768 0.0782768	0.000 0.000	1.340162 0.896638	1.728324 1.284800
		3.0000		dimension3	1.0000 2.0000	0.4435245* −1.0907186*	0.0782768 0.0782768	0.000 0.000	0.249443 −1.284800	0.637605 −0.896638
ACO3	dimension2		1.0000	dimension3	2.0000 3.0000	−0.6871487* −0.3191597*	0.0545407 0.0545407	0.000 0.000	−0.822378 −0.454389	−0.551920 −0.183931
		2.0000		dimension3	1.0000 3.0000	0.6871487* 0.3679890*	0.0545407 0.0545407	0.000 0.000	0.551920 0.232760	0.822378 0.503218
		3.0000		dimension3	1.0000 2.0000	0.3191597* −0.3679890*	0.0545407 0.0545407	0.000 0.000	0.183931 −0.503218	0.454389 −0.232760
SMOX	dimension2		1.0000	dimension3	2.0000 3.0000	−1.0486278* −0.7268455*	0.0303457 0.0303457	0.000 0.000	−1.123868 −0.802085	−0.973388 −0.651606
		2.0000		dimension3	1.0000 3.0000	1.0486278* 0.3217822*	0.0303457 0.0303457	0.000 0.000	0.973388 0.246542	1.123868 0.397022
		3.0000		dimension3	1.0000 2.0000	0.7268455* −0.3217822*	0.0303457 0.0303457	0.000 0.000	0.651606 −0.397022	0.802085 −0.246542

* The significance level of mean difference was 0.05; SE – standard error; 95% CI – 95% confidence interval; HSD – honestly significant difference.

to vascular endothelial cells, and produces NO, which affects the permeability of blood vessels and increases damage to retinal cells. The original statistical data of PCR are shown in Table 2–5.

Discussion

The occurrence and development of DR is a complex pathological process, and a series of pathological changes of DR are caused by abnormal changes of cytokines, signal transduction metabolic enzymes, inflammation, ion channels, and related genes.[17,18] Neovascularization is a characteristic pathological marker of the entry of DR into the proliferative phase. Therefore, preventing and inhibiting the formation of DR neovascularization is a key target to delay the progression of DR. The PI3K/Akt signaling pathway is one of the signaling pathways that participate in the regulation of cell growth, proliferation and differentiation.[19,20] When the PI3K/Akt signaling pathway is activated, it can not only accelerate the survival cycle of endothelial cells, but also cooperate with VEGF in cell survival and migration, and finally induce the formation of new blood vessels.[21] The AKT regulates serine antiapoptotic signaling protein in endothelial cells from cell cycle G1 phase to S phase. Therefore, AKT regulates endothelial cell proliferation, migration and has a key role in inducing angiogenesis.[22,23] In this study, the ischemia and hypoxia

Table 4. Normality test

Genes	Groups		Kolmogorov–Smirnov[a]			Shapiro–Wilk		
			statistics	df	Sig.	statistics	df	Sig.
ANGPT1	dimension1	1.0000	0.162	10	0.200*	0.943	10	0.592
		2.0000	0.238	10	0.115	0.874	10	0.113
		3.0000	0.155	10	0.200*	0.920	10	0.358
ANGPT4	dimension1	1.0000	0.162	10	0.200*	0.967	10	0.858
		2.0000	0.200	10	0.200*	0.946	10	0.625
		3.0000	0.145	10	0.200*	0.950	10	0.665
KDR	dimension1	1.0000	0.180	10	0.200*	0.936	10	0.512
		2.0000	0.184	10	0.200*	0.920	10	0.355
		3.0000	0.209	10	0.200*	0.835	10	0.038
AKT	dimension1	1.0000	0.202	10	0.200*	0.892	10	0.179
		2.0000	0.149	10	0.200*	0.951	10	0.680
		3.0000	0.258	10	0.058	0.870	10	0.101
ACO3	dimension1	1.0000	0.257	10	0.060	0.894	10	0.186
		2.0000	0.170	10	0.200*	0.947	10	0.636
		3.0000	0.163	10	0.200*	0.981	10	0.972
SMOX	dimension1	1.0000	0.169	10	0.200*	0.909	10	0.275
		2.0000	0.182	10	0.200*	0.918	10	0.344
		3.0000	0.244	10	0.094	0.908	10	0.269

a – Lilliefors significant level correction; * The lower limit of the true significance level; df – degrees of freedom.

induced by high glucose level in the rat model activated and accelerated the expression of AKT in the PI3k/Akt signaling pathway, and increased its phosphorylation, thus accelerating the formation of neovascularization. The results of this experiment showed that the expression of AKT and related proteins in the DR group and anti-ACO3 group was significantly higher than in the control group, indicating that the expression of AKT was enhanced and the PI3k/Akt signaling pathway was activated during the formation of DR lesions.

Limitations of the study

This study is mainly based on the basic experiment of animal model. It explored the involvement of ACO3 protein in DR through the PI3k/Akt signaling pathway of rat model of DR. However, there are still great structural and pathological differences between animals and humans. Therefore, this study should also examine the differences and effects of various animal models, and further clinical studies should be performed.

Conclusions

As an important pathway involved in endothelial cell migration, proliferation and vascular dysfunction, the PI3K/Akt signaling pathway also plays an important role in the process of DR neovascularization. The ACO3 protein, also known as VAP1, is involved in regulating cell proliferation and inducing neovascularization.[24] Proteins ACO3 and SMOX have the characteristics of mutual regulation, and are synergistically involved in the regulation of amino acid metabolism.[25] The expression levels of ACO3, SMOX and AKT proteins were decreased in the anti-ACO3 group, which indicated that the PI3K/Akt signaling pathway was inhibited, and the formation of retinal neovascularization was inhibited to a certain extent. This delayed the progression of DR and played a certain therapeutic role in the proliferation phase.

ORCID iDs

Yi Zhang https://orcid.org/0000-0003-0536-9643
Wenjun Wang https://orcid.org/0000-0001-8725-6233
Anhuai Yang https://orcid.org/0000-0001-7429-277X

References

1. Hendrick AM, Gibson MV, Kulshreshtha A. Diabetic retinopathy. *Prim Care*. 2015;42(3):451–464. doi:10.1016/j.pop.2015.05.005
2. Ruta LM, Magliano DJ, Lemesurier R, Taylor HR, Zimmet PZ, Shaw JE. Prevalence of diabetic retinopathy in type 2 diabetes in developing and developed countries. *Diabet Med*. 2013;30(4):387–398. doi:10.1111/dme.12119
3. Thapa R, Bajimaya S, Sharma S, Rai BB, Paudyal G. Systemic association of newly diagnosed proliferative diabetic retinopathy among type 2 diabetes patients presented at a tertiary eye hospital of Nepal. *Nepal J Ophthalmol*. 2015;7(13):26–32. doi:10.3126/nepjoph.v7i1.13163
4. Song P, Yu J, Chan KY, Thodoratou E, Rudan I. Prevalence, risk factors and burden of diabetic retinopathy in China: A systematic review and meta-analysis. *J Glob Health*. 2018;8(1):010803. doi:10.7189/jogh.08.010803
5. Wang W, Lo ACY. Diabetic retinopathy: Pathophysiology and treatments. *Int J Mol Sci*. 2018;19(6):1816. doi:10.3390/ijms19061816

Table 5. All original data of Fig. 4 and Fig. 5 (normal group 1, diabetic retinopathy (DR) group 2, anti-ACO3 group 3)

Groups	ANGPT1	ANGPT4	KDR	AKT	ACO3	SMOX
1.0000	0.3751	0.3681	0.4012	1.1859	1.5135	0.8563
1.0000	0.3797	0.3630	0.4306	1.1366	1.5435	0.8793
1.0000	0.3442	0.3807	0.4442	1.0718	1.6208	0.7934
1.0000	0.3124	0.3815	0.4606	0.9978	1.5258	0.7756
1.0000	0.3361	0.3855	0.4583	0.9030	1.5464	0.7111
1.0000	0.3146	0.4037	0.4243	0.8884	1.5170	0.7290
1.0000	0.3368	0.3651	0.4156	0.9092	1.4031	0.7661
1.0000	0.3684	0.3295	0.4103	0.9118	1.3439	0.7236
1.0000	0.4032	0.3490	0.4461	0.9965	1.3493	0.7403
1.0000	0.4382	0.3766	0.4528	0.9812	1.3810	0.6958
2.0000	1.5104	1.3320	1.3188	2.6577	2.5062	1.8124
2.0000	1.4524	1.4466	1.2353	2.8856	2.2577	1.9028
2.0000	1.5086	1.5247	1.3260	2.7656	2.2703	1.8016
2.0000	1.6421	1.4825	1.3847	2.7385	2.0583	1.7821
2.0000	1.6139	1.3622	1.3804	2.6138	2.1176	1.7776
2.0000	1.5291	1.2285	1.3708	2.4437	1.9295	1.8797
2.0000	1.6609	1.2603	1.2588	2.3809	2.1160	1.8946
2.0000	1.8085	1.3353	1.3020	2.2655	2.0146	1.8209
2.0000	1.9824	1.3035	1.2217	2.3728	2.1738	1.6795
2.0000	2.1072	1.3465	1.4007	2.2005	2.1720	1.8055
3.0000	0.5871	0.5133	0.5087	1.5631	1.9046	1.5839
3.0000	0.5946	0.4715	0.4947	1.6333	1.8093	1.4745
3.0000	0.5418	0.4444	0.5353	1.5854	1.9456	1.4716
3.0000	0.5169	0.4306	0.5393	1.5326	1.8286	1.3850
3.0000	0.4756	0.3888	0.5091	1.5533	1.8504	1.4733
3.0000	0.4622	0.3648	0.5001	1.5094	1.7161	1.5046
3.0000	0.4294	0.3802	0.4947	1.3700	1.6973	1.4477
3.0000	0.4290	0.4171	0.5387	1.2463	1.8135	1.4429
3.0000	0.4578	0.4103	0.5398	1.2503	1.7495	1.5029
3.0000	0.5019	0.4010	0.5296	1.1740	1.6211	1.6525

6. Park HC, Lee YK, Cho A, et al. Diabetic retinopathy is a prognostic factor for progression of chronic kidney disease in the patients with type 2 diabetes mellitus. *PLoS One*. 2019;14(7):e0220506. doi:10.1371/journal.pone.0220506

7. Semeraro F, Morescalchi F, Cancarini A, Russo A, Rezzola S, Costagliola C. Diabetic retinopathy, a vascular and inflammatory disease: Therapeutic implications. *Diabetes Metab*. 2019;45(6):517–527. doi:10.1016/j.diabet.2019.04.002

8. Piao CL, Luo JL, Jin D, et al. Utilizing network pharmacology to explore the underlying mechanism of *Radix salviae* in diabetic retinopathy. *Chin Med*. 2019;14:58. doi:10.1186/s13020-019-0280-7

9. Xiao YL, Feng X. Mechanism of NLRP3/IL-1β pathway in the progression of diabetic retinopathy [in Chinese]. *Int Eye Sci*. 2019;19(9):1559–1562. http://www.ijo.cn/cn_publish/2019/9/201909026.pdf.

10. Solomon SD, Chew E, Duh EJ, et al. Diabetic retinopathy: A position statement by the American Diabetes Association. *Diabetes Care*. 2017;40(3):412–418. doi:10.2337/dc16-2641

11. He J, Qiu Y, Zhou X. A study of Na(+)-K(+)-ATPase activity in erythrocyte membrane from diabetic retinopathy patients [in Chinese]. *Zhonghua Yan Ke Za Zhi*. 1998;34(6):421–423. PMID:11877243.

12. Li H, Luo XX, Feng YP, Wang H. Effects of a traditional Chinese patent medicine for PI3K/Akt pro-survival signal channel in diabetic retinopathy rat. *Int Eye Sci*. 2016;16(12):2195–2199. doi:10.3980/j.issn.1672-5123.2016.12.06

13. Huali Z, Jing G, Zhe X, et al. A comparative study of fundus photography and fluorescein fundus angiography in the diagnosis of diabetic retinopathy in Tibetans [in Chinese]. *Sichuan Medical Journal*. 2019;7(40):726–728.

14. Guo D, Du N. Therapeutic effect and mechanism of paclitaxel on diabetic retinopathy model rats. *Int Eye Sci*. 2019;19(12):2026–2030. doi:10.3980/j.issn.1672-5123.2019.12.06

15. Zafirovic S, Sudar-Milovanovic E, Obradovic M, et al. Involvement of PI3K, Akt and RhoA in oestradiol regulation of cardiac iNOS expression. *Curr Vasc Pharmacol*. 2019;17(3):307–318. doi:10.2174/1570161116666180212142414

16. Rouhani F, Khodarahmi P, Naseh V. NGF, BDNF and Arc mRNA expression in the hippocampus of rats after administration of morphine. *Neurochem Res*. 2019;44(9):2139–2146. doi:10.1007/s11064-019-02851-z

17. Radha V, Rema M, Mohan V. Genes and diabetic retinopathy. *Indian J Ophthalmol*. 2002;50(1):1–5. PMID:12090088.

18. Fleissig E, Adhi M, Sigford DK, Barr CC. Foveal vasculature changes and nonperfusion in patients with diabetes types I and II with no evidence of diabetic retinopathy. *Graefes Arch Clin Exp Ophthalmol*. 2020;258(3):551–556. doi:10.1007/s00417-019-04588-5

19. Tao D. PI3K-AKT pathway and diabetic optic reticulum lesions [in Chinese]. *World Latest Medicine Information*. 2016;16(44):34–35.

20. Koga T, Suico MA, Shimasaki S, et al. Endoplasmic reticulum (ER) stress induces Sirtuin 1 (SIRT1) expression via the PI3K-Akt-GSK3β signaling pathway and promotes hepatocellular injury. *J Biol Chem*. 2015;290(51):30366–30374. doi:10.1074/jbc.M115.664169

21. Campo L, Turley H, Han C, et al. Angiogenin is up-regulated in the nucleus and cytoplasm in human primary breast carcinoma and is associated with markers of hypoxia but not survival. *J Patholog*. 2005;205(5):585–591. doi:10.1002/path.1740

22. Song Q, Han CC, Xiong XP, et al. PI3K-Akt-mTOR signal inhibition affects expression of genes related to endoplasmic reticulum stress. *Genet Mol Res*. 2016;15(3):1–8. doi:10.4238/gmr.15037868

23. Li S, Li Q, Yu W, Xiao Q. High glucose and/or high insulin affects HIF-1 signaling by regulating AIP1 in human umbilical vein endothelial cells. *Diabetes Res Clin Pract*. 2015;109(1):48–56. doi:10.1016/j.diabres.2015.05.005

24. Wang H, Clainche AL, Dall MTL, et al. Cloning and characterization of the peroxisomal acyl CoA oxidase *ACO3* gene from the alkane-utilizing yeast *Yarrowia lipolytica*. *Yeast*. 1998;14(15):1373–1386. doi:10.1002/(SICI)1097-0061(199811)14:15<1373::AID-YEA332>3.0.CO;2-1

25. Fan J, Chen M, Wang X, et al. Targeting Smox is neuroprotective and ameliorates brain inflammation in cerebral ischemia/reperfusion rats. *Toxicol Sci*. 2019;168(2):381–393. doi:10.1093/toxsci/kfy300